

## FLUID DYNAMIC GAUGING FOR PULSED FLOW CLEANING

N. Gottschalk\*, S. Foisel, F. Schlüter, W. Augustin and S. Scholl

Technische Universität Braunschweig, Institute for Chemical and Thermal Process Engineering,  
Langer Kamp 7, 38106 Braunschweig, Germany

\* Corresponding author: n.gottschalk@tu-braunschweig.de

### ABSTRACT

Fluid Dynamic Gauging (FDG) is a non-contact distance measurement technique and can be used to determine the thickness of fouling layers in stationary liquid flows. In order to monitor the deposit removal during pulsed flow cleaning processes, this technique was transferred to non-stationary flows. To proof the applicability three important parameters were investigated experimentally:

- Influence of the measurement period on the mass flow rate determination,
- Characteristics of correlation between discharged mass flow rate and the distance of the nozzle tip to the gauged surface,
- Accuracy of distance measurements depending on the waviness of the pulsed flow.

Measurements were performed in a test rig with annular cross section on a clean surface at different stationary and transient flow velocities.

Although the discharged mass flow rate through the nozzle was significantly oscillating, the applicability of FDG in pulsed flows could be shown. However, there are some pulsed flow characteristics, which require attention before conducting measurements.

### INTRODUCTION

The formation of fouling, e.g. on heated surfaces, is still a severe problem in food processing. Fouling layers often decrease the thermal efficiency of heat exchangers due to the additional thermal resistance. In order to ensure high hygiene and food safety requirements, production lines in food industry must be cleaned thoroughly and regularly. As this is not possible during production processes, economically expensive cleaning breaks are necessary. Thereby, costs arise also for detergents (purchase and disposal), rinse water and energy. Therefore, enhancing cleaning processes is an important aspect to optimize production processes economically as well as ecologically.

In industrial cleaning-in-place (CIP) several cleaning steps are performed for a prescribed time, at a certain temperature, flow rate and chemical concentration (Goode et al. 2013). However, a variety of different mechanisms is involved in the removal of soils and far not all important aspects are yet understood. For closed equipment, e.g. pipes,

plate-and-frame or tubular heat exchangers, the general factors of influence in cleaning procedures can be described with the extended Sinner circle specifying several parameters (Dürr and Wildbrett, 2006). These are the type, condition and amount of soil, as well as design, material and roughness of the surface. Furthermore, temperature, chemistry, mechanics and time are relevant parameters of the cleaning solution.

The flow velocity of the cleaning solution is a key parameter in almost all cleaning processes. An increased flow velocity leads to a decreased thickness of the laminar sublayer and a higher wall shear stress (Dürr and Wildbrett, 2006). Fryer and Asteriadou (2009) categorized three different types of deposits: viscous liquids removed with hot water, cohesive soils removed with chemicals and biofilms. Goode et al. (2013) compared several cleaning studies and stated decreasing cleaning times with increasing shear rates especially for viscous liquids and cohesive soils.

The enhancement of cleaning processes by using pulsed flows is reported in several papers. Gillham et al. (2000) stated increasing cleaning and removal rates for whey protein foulants in alkaline pulsed flows. Bode et al. (2007) discovered a huge influence of the ratio between maximum oscillating and mean flow velocity on whey protein cleaning. Cleaning enhancement in complex geometries, like abrupt extensions and curved pipes, using pulsed flows is reported from Augustin et al. (2010). Föste et al. (2013) developed a CFD (computational fluid dynamics) model for pulsed flow cleaning of mass-transfer-controlled fouling systems. Schöler et al. (2009) presented investigations on the removal of starch layers during pulsed flow cleaning using a measuring technique based on phosphorescence detection with a CCD (charge-coupled device) camera. With this technique the necessary cleaning time for total removal of deposits can be determined with local resolution, but measuring the deposit thickness and its temporal change during pulsed flow cleaning is not possible. Fluid Dynamic Gauging (FDG) could be an alternative for further investigation, if this technique was applicable in non-stationary flows.

This work presents experimental investigations on the applicability of FDG in pulsed flows and its limitations. To proof the applicability of FDG, three important parameters were examined experimentally: the influence of measurement period, the characteristics of calibration curves and the accuracy of distance measurements. Measurements were

performed in a test rig with an annular cross section on a clean surface at different stationary and transient flow velocities.

## FUNDAMENTALS

### Pulsed Flow Cleaning

Pulsed flows consist of a stationary flow  $w_{stat}$  with a superimposed sinusoidal oscillating fluid movement  $w_{os}$ . The intensity of the pulsation can be quantified by the ratio of the maximum oscillating flow velocity  $w_{os,max}$  and the mean flow velocity  $\bar{w}$ . This dimensionless value is called waviness  $W$ .

$$W = \frac{w_{os,max}}{\bar{w}} \quad (1)$$

The mean flow velocity  $\bar{w}$  for an oscillation interval  $t_{os}$  is defined as follows:

$$\bar{w} = \frac{1}{t_{os}} \int_0^{t_{os}} w(t) dt \quad (2)$$

with the unsteady velocity:

$$w(t) = w_{stat} + w_{os} = w_{stat} + w_{os,max} \cdot \sin(\omega t) \quad (3)$$

For wavinesses  $W > 1$  a temporary flow reversal occurs in the proximity of the wall (Schlichting and Gersten, 2006), as shown in Fig. 1. At higher waviness a separation of the viscous sublayer and formation of eddies is believed to be likely. This would lead to a decrease of the laminar sublayer thickness at turbulent flows. Since the ratio of inertial and frictional forces is variable, the annular effect is specific for pulsed flows. Hence, the temporary maximum velocity does not necessarily occur in the center of the pipe, but can also occur near the wall. This results in large shear rates and high wall shear stresses. (Bode et al., 2007; Augustin et al., 2010)

Bode et al. (2007) published cleaning experiments of whey protein fouling and reported a decrease in cleaning time with increasing waviness, see Fig. 2. The total cleaning time  $\tau_M$  was reduced from approx. 24 min at stationary flow to 10 min at  $W = 4$ . Also noticeable is the sudden drop at the waviness  $W = 1$ , which is presumably due to a beginning flow reversal in the proximity of the wall. (Bode et al., 2007)

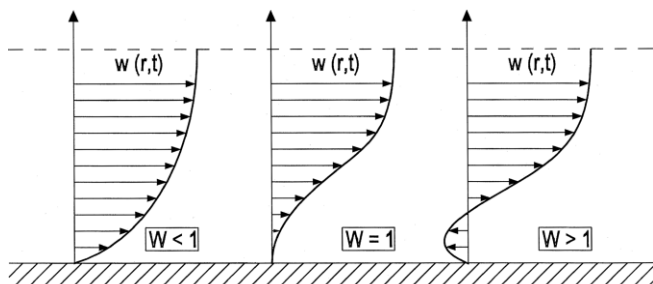


Fig. 1 Velocity profiles of pulsed flows depending on waviness (Augustin and Bohnet, 1999).

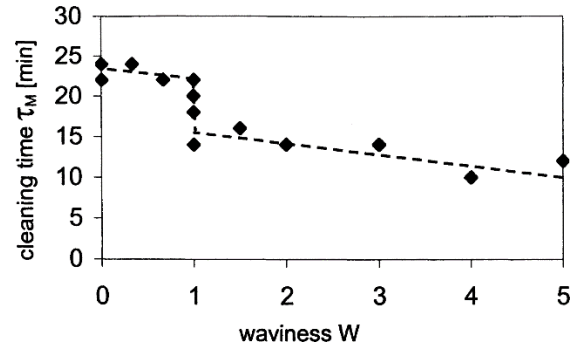


Fig. 2 Effect of waviness on total cleaning time of whey protein deposits at pH 12 and  $T = 18^\circ\text{C}$  (Bode et al., 2007)

### Fluid Dynamic Gauging

Fluid Dynamic Gauging (FDG) is a non-contact technique to measure the thickness of fouling deposits in-situ in a liquid environment and was developed by Tuladhar et al. (2000). Gu et al. (2009; 2011) transferred the technique to an annular geometry and showed the suitability for curved surfaces.

The measuring principle is based on liquid flow through the nozzle caused by a constant pressure difference, called fixed suction mode (Gu et al., 2011). The hydrostatic pressure difference can be calculated from the difference in height between the nozzle tip and the discharge end of the gauge. Within a certain measuring range the discharged mass flow rate  $\dot{m}$  is uniquely related to the distance between the tip of the nozzle and the gauging surface  $h$ , e.g. a fouling layer. Using a calibration curve,  $h$  can be calculated from  $\dot{m}$ , thus detection of increase or decrease of the fouling layer thickness is possible. Usually  $h$  is divided by the nozzle throat diameter  $d_t$  to calculate the dimensionless distance  $h/d_t$ , which is used for creating nozzle independent calibration curves. The fouling layer thickness  $\delta$  can be calculated from  $h$  and the distance between the nozzle and the substrate  $h_0$ . Measurements are possible in stationary liquids (e.g. tanks) for laboratory analysis and in stationary flows (e.g. pipes). The applicability of FDG measurements in discontinuous, like pulsed flows is not reported so far.

Besides the fixed suction mode FDG, measurements are alternatively possible in the fixed gauging flow mode. Thereby the mass flow rate is maintained at a constant level and the pressure drop across the nozzle is measured (Gu et al., 2011). This mode is especially useful for investigations under aseptic conditions or in small tanks, where less fluid is available (Wang et al., 2016).

## EXPERIMENTS

### Experimental Setup

The main parts of the fouling and cleaning test rig are a tank, two pumps, a heat exchanger and a measuring section, see Fig. 3. The heated storage tank for protein or cleaning solution is stirred to compensate concentration gradients. The stationary flow velocity is generated by a high-pressure

pump, while a reciprocating pump with shut suction side serves as pulsator. The amplitude of the velocity pulse can be adjusted by variation of the piston stroke. A plate heat exchanger with cooling water on the service side guarantees constant temperature during cleaning experiments.

The annular measuring section is located vertically with liquid flowing upwards. The heating rod (316 stainless steel,  $d = 14$  mm) is 430 mm long. The surface temperature of the rod  $T_w$  is measured with three thermocouples 1.5 mm underneath the surface. The heat flux  $\dot{q}$  is controlled by the preset power input (7 ... 78 kW/m<sup>2</sup>). Thermocouples located at the in- and outlet of the measuring section are used to determine the bulk liquid temperature  $T_{bulk}$ . The outer pipe is acrylic with an inner diameter of 30 mm and an integrated FDG nozzle.

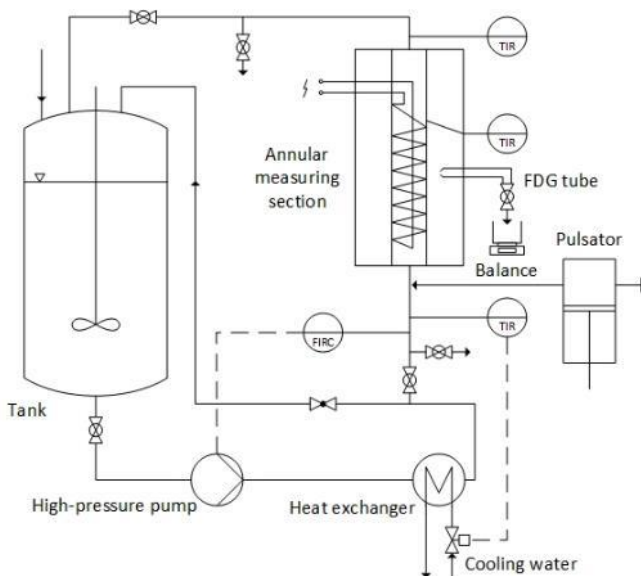


Fig. 3 Schematic of fouling and cleaning test rig

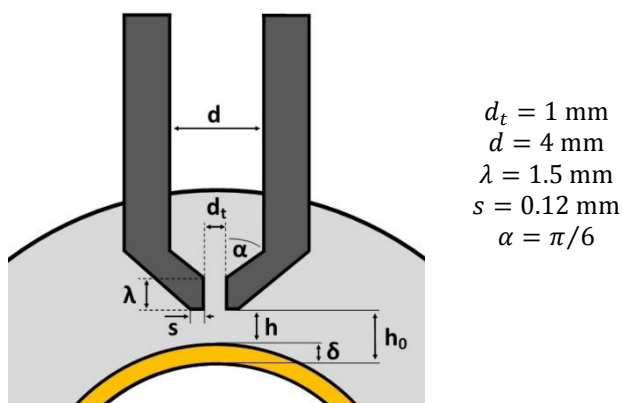


Fig. 4 Schematic of fluid dynamic gauge in annular geometry. Symbols:  $d_t$  – inner diameter of nozzle;  $d$  – inner tube diameter;  $\lambda$  – length of nozzle exit;  $s$  – width of nozzle rim;  $\alpha$  – nozzle inner angle;  $h$  – distance between nozzle tip and deposit layer,  $h_0$  – distance between nozzle tip and substrate surface;  $\delta$  – thickness of deposit layer.

The FDG nozzle (dimensions see Fig. 4) is fabricated from 316 stainless steel and is located normal to the heating rod surface. The distance between the tip of the nozzle and the surface of the heating rod  $h_0$  is adjusted with a micrometer screw. A vertical tube ( $l = 393$  mm) is connected to the gauging nozzle with a valve at the other end, which is open to atmosphere. The discharge mass flow rate  $\dot{m}$  is measured using an electronic balance (accuracy  $\pm 0.05$  g).

### Applicability of FDG in Pulsed Flows

To show the applicability of the FDG technique in pulsed flows, preliminary tests were performed with water and a clean heating rod. Experiments were carried out at 12 different flow conditions: three stationary and four maximum oscillating flow velocities, resulting in 9 different non-zero wavinesses, see Table 1.

Table 1. Wavinesses at investigated flow conditions

Waviness $W$ [-]	Stationary flow velocity $w_{stat}$ [m/s]	Max. oscillating flow velocity $w_{os,max}$ [m/s]			
		0	0.40	0.48	0.55
0.36	0	1.1	1.3	1.5	
	0.50	0.8	1.0	1.1	
	0.80	0.5	0.6	0.7	

### Influence of measurement period

The influence of the measurement period on the accuracy of mass flow rate determination was investigated at the dimensionless distance  $h/d_t = 0.1$  for all flow conditions. The discharged masses after different measurement periods ( $t_m = 15$  s; 30 s; 60 s; 90 s) were determined and the uncertainty of mass flow rate measurements  $u_m$  between 15 measurements were assessed and divided by the average mass flow rate to determine the percental measurement uncertainty.

The uncertainty of mass flow rate measurements  $u_m$  decreases with longer measurement periods at all investigated flow conditions, exemplarily shown for  $w_{stat} = 0.50$  m/s in Fig. 5. This is particularly obvious for stationary flows ( $W = 0$ , no pulse), since higher discharged liquid masses can be determined more accurately and inaccuracies in the measurement conduct, like stopping the measurement period, have less influence.

For pulsed flows ( $W > 0$ ) the uncertainty does not follow a monotonous decrease with measurements periods and in contrast seems to slightly increase between measurement periods of 60 s and 90 s. This effect is not understood yet and needs further investigation. Since a short measuring period is preferable for a higher temporal resolution and the uncertainty of mass flow rate measurements at 60 s is low enough, all following experiments were performed with a measurement period of 60 s.

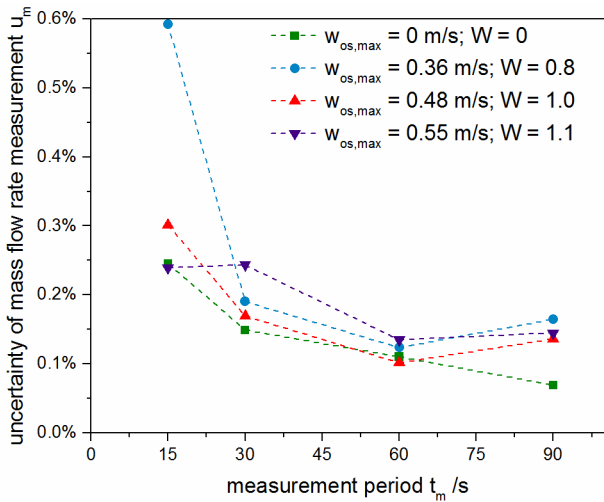


Fig. 5 Influence of the measurement period  $t_m$  on the accuracy of mass flow rate measurement at  $h/d_t = 0.1$  and different flow conditions ( $w_{stat} = 0.50$  m/s).

#### Characteristics of calibration curves

In order to investigate the characteristics of correlation between discharge mass flow rate  $\dot{m}$  and the distance of the nozzle tip to the gauging surface  $h$ , calibration curves were recorded at different flow conditions (Table 1). For this, the discharge mass flow rate was determined three times at dimensionless distances between  $h/d_t = 0.02$  and  $0.04$  and for stationary flows additionally at  $h/d_t = 0$ .

Calibration curves in stationary flows always increase almost linear at low dimensionless distances and converge to an asymptotic mass flow rate, see Fig. 6. This correlation was fitted by the sigmoidal Boltzmann function with the constants  $B_0$ ,  $B_e$ ,  $x_c$  and  $dx$ , listed in Table 2:

$$\dot{m} = B_e + (B_0 - B_e) \left( 1 + e^{\frac{h}{d_t} - x_c} \right)^{-1} \quad (4)$$

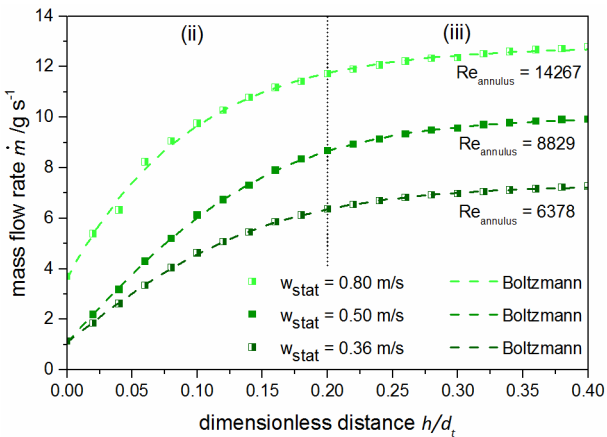


Fig. 6 Calibration curves, measured data points and fitted curves, in stationary flows ( $W = 0$ ) at different stationary flow velocities. Regions marked: (ii) incremental zone, (iii) asymptotic zone.

Table 2. Constants for Boltzmann fit of calibration curves in stationary flows

$w_{stat}$ [m/s]	$B_0$ [g/s]	$B_e$ [g/s]	$x_c$	$dx$	$R^2$
0.36	-6.231	7.306	-0.014	0.083	1.000
0.50	-7.598	10.020	0.002	0.080	1.000
0.80	-219.454	12.799	-0.290	0.091	0.997

The constants are dependent on the nozzle throat diameter  $d_t$ , the fluid density  $\rho$  and the pressure difference over the nozzle  $\Delta P$ , which is influenced by the flow velocity in the annulus.

The calibration curves of stationary flows ( $W = 0$ ), see Fig. 6, show comparable curve shapes as reported by Gu et al. (2011), shown in Fig. 7. Gu et al. (2011) stated three zones of calibration curves: (i) curvature, (ii) incremental and (iii) asymptotic zone, see Fig. 7. The incremental and asymptotic zone are marked in Fig. 6, but the existence of a curvature zone is not apparent. The expressiveness of this zone depends for example on the relation between the nozzle throat size and the rod diameter (Gu et al., 2011). Furthermore, the size of the curvature zone also seems to decrease with increasing flow velocities, as at  $Re_{annulus} = 10,000$  its existence is not obvious, see Fig. 7.

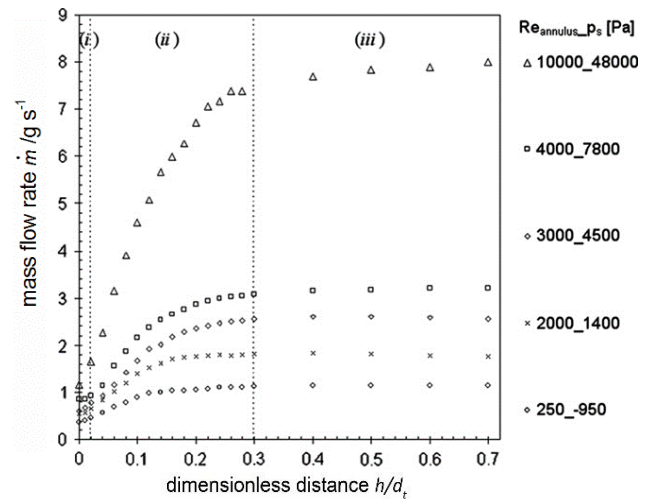


Fig. 7 Calibration curves in stationary flows at different Reynolds numbers and corresponding pressure. Regions marked: (i) curvature zone, (ii) incremental zone, (iii) asymptotic zone. (adapted from Gu et al., 2011).

Higher stationary flow velocities generally lead to higher mass flow rates through the nozzle. This is particularly obvious in the asymptotic region, see Fig. 6. Here, the mass flow rate increases from  $\dot{m} = 7.3$  g/s at  $Re_{annulus} = 6,378$  to  $\dot{m} = 12.8$  g/s at  $Re_{annulus} = 14,267$ . These mass flow rates are slightly higher than determined by Gu et al. (2011) in a similar experimental setup.

The mass flow rate at  $h/d_t = 0$  reaches not zero, because there is always a gap between the curved gauging surface and the flat nozzle tip (Gu et al., 2011). For stationary

flow conditions the working range for the gauge is  $0 \leq h/d_t \leq 0.2$ . In this range the mass flow rate is sensitive enough to  $h/d_t$ .

At small dimensionless distances the mass flow rate is less sensitive to increasing stationary flow velocities than in the asymptotic region. Therefore the gradient increases with higher flow velocities and allows a more accurate determination of the distance between nozzle tip and gauged surface.

The calibration curves for stationary and pulsed flows are shown in Fig. 8. The general curve shape of the calibration curves is not influenced by applying pulsation. They also consist of an incremental and an asymptotic zone. The curvature zone, if existent, is not detectable as measurements at smaller dimensionless distances as  $h/d_t = 0.02$  are not possible due to vibrations of the heating rod, introduced by the pulsed flow. The working range for pulsed flows is  $0.02 \leq h/d_t = 0.2$  and is thereby nearly identical to the working range in stationary flows.

The overall influence of the pulsation on calibration curves is significantly smaller than the influence of the stationary flow velocity. This is obvious looking at the gradient in the incremental zone and the size of the mass flow rate at the asymptotic zone. Nevertheless, comparing the calibration curves at the same stationary flow velocity, an influence of pulsation becomes apparent.

The influence of the waviness on the calibration curve depends, besides the absolute value, also on the stationary flow velocity. Calibration curves for  $W > 1$  at  $w_{stat} = 0.36$  m/s show a smaller mass flow rate with increasing waviness, especially in the asymptotic area but also at small  $h/d_t$ , see Fig. 8a. All calibration curves at  $w_{stat} = 0.50$  m/s in Fig. 8b show the same behavior in the asymptotic area.

However, at  $W = 1.1$  and small  $h/d_t$  the mass flow rate is higher than at stationary flow condition, although the waviness is similar to one of the previous experiments. This behavior might be caused by a measurement error, although the measurement was repeated twice with similar results. Nevertheless, the temporarily high maximum flow velocity ( $w_{max} = 1.05$  m/s) causes vibrations of the heating rod, which can influence the measurement. Furthermore, the determination of zero nozzle position, i.e. heating rod surface, is rather inaccurate. This leads to differences between the adjusted distance and the real distance during the measurement. Therefore, further experiments and probably simulations are needed to gain a better understanding of the influences of  $W > 1$  on the calibration curves.

At the highest stationary flow velocity ( $w_{stat} = 0.80$  m/s) the waviness has only minor influence on the calibration curves. The investigated wavinesses are rather small and thus lead to small differences in the maximum flow velocities related to the stationary flow velocity.

#### Accuracy of distance measurement

To investigate the accuracy of distance measurements by FDG in pulsed flows, the mass flow rate at  $h/d_t = 0.1$  at different flow conditions was measured 15 times. Thereby the nozzle distance was adjusted only once for each flow condition. The distance  $h$  was then calculated for each mass

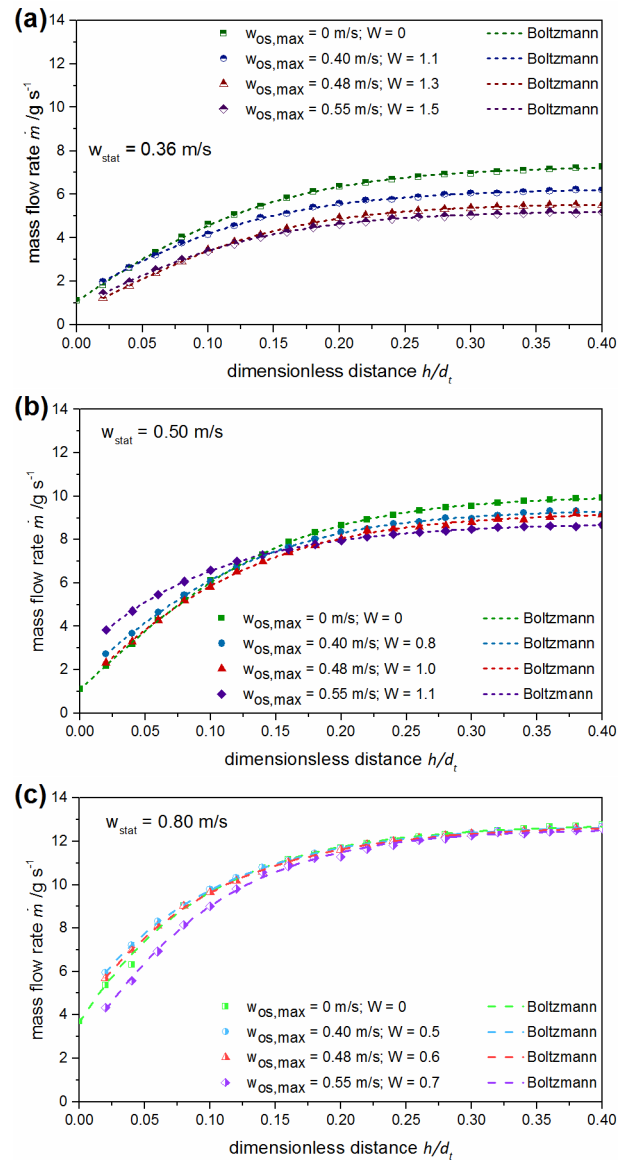


Fig. 8 Calibration curves, measured data points and fitted curves, at different flow conditions. (a)  $w_{stat} = 0.36$  m/s. (b)  $w_{stat} = 0.50$  m/s. (c)  $w_{stat} = 0.80$  m/s.

flow rate using the previously determined calibration curves. The average deviation from the calculated to the adjusted distance is a measure for the measurement accuracy and shown in Fig. 9 for all flow conditions. Error bars indicate standard deviations between the 15 measurements.

The standard deviations within the 15 repetitions are very small, as indicated by the error bars. However, the overall uncertainty with respect to distance determination for all experimental settings is  $\pm 43$   $\mu\text{m}$ . The waviness seems to have no influence on the deviation, as the highest deviation between calculated and adjusted distance occurs at  $W = 0$  and  $w_{stat} = 0.36$  m/s. This is particularly noticeable since the mass flow rate through the nozzle is non-stationary at pulsed annular flows. This does not seem to influence the measurement accuracy, at least at an adequate high measurement period.

Different aspects may contribute to the inaccuracy of the distance measurement. A poor representation of the data points by the calibration curve would lead to errors, for example. Since the determined calibration curves show good agreement with the measured mass flow rates at  $h/d_t = 0.1$ , see Fig. 8, this is not the case.

Alternatively, an inaccurate adjusted distance of the nozzle tip to the gauging surface  $h$  can lead to differences in distance measurements. This presumption is supported by significant differences in the measured mass flow rate of two experiments, which each newly adjusted  $h$ . The adjustment of  $h$  can easily be inaccurate as the nozzle is moved by a micrometer screw and the position cannot be adjusted more accurately than  $\pm 10 \mu\text{m}$ . This inaccuracy can easily be reduced by changing the nozzle movement system, for example by using a step motor.

Besides the inaccuracy caused by the nozzle movement, the accuracy of zero nozzle position determination has a large influence on the preciseness of the distance measurement. The zero position is determined by moving the nozzle slowly closer to the rod until the contact is manually noticeable. Thereby, it occurs easily that the heating rod is slightly pushed away and the zero position is not determined accurately. To enable a more precise zero position determination, the lateral movement of the heating rod must be inhibited and a better detection of the contact between nozzle tip and rod surface is needed. One possibility for this is using an electrical circuit at low voltage, which is closed by the contact between nozzle and rod. The closure of an electrical circuit can easily be measured and thus strongly increases the zero nozzle position determination.

Unfortunately, this technique cannot be used in liquid environment. Therefore, the determination of zero nozzle position can only be conducted in air and thus at room temperature, which is adequate for measurements at low bulk temperatures, but might influence the accuracy for measurements at higher liquid temperatures.

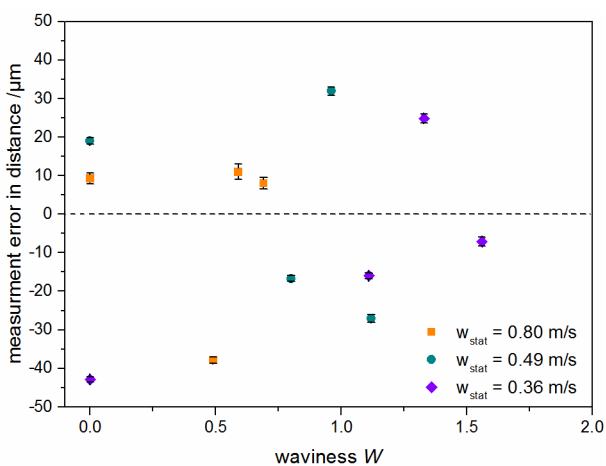


Fig. 9 Distance measurement deviation at different flow conditions and  $h/d_t = 0.1$ .

Despite the inaccuracy at the distance measurements, FDG can be used in pulsed flows. Although, the used nozzle movement system is not accurate enough to determine

absolute deposit thicknesses, it still might be appropriate to investigate the relative change in deposit thickness over time. This is especially important for monitoring cleaning processes.

## CONCLUSIONS

The applicability of Fluid Dynamic Gauging (FDG) measurement in pulsed flows has been shown. An accurate distance determination from the discharged mass flow rate is possible, but requires attention to some pulsed flow characteristics. The measuring period should be chosen as high as possible within the needed temporal resolution, as the uncertainty of the mass flow rate measurement decreases with increasing measurement period. Moreover, a precise calibration at the applied flow conditions, stationary and maximum oscillating flow velocity, is necessary, since only an accurate mathematical description of the correlation between the discharged mass flow rate and the dimensionless distance allows a precise calculation of the distance during cleaning experiments. Furthermore, the accuracy of distance measurements is not significantly influenced by the waviness, but the used nozzle movement system and the depicted determination of the zero nozzle position lead to an increased uncertainty in distance measurements. The first issue can be solved by using a more accurate adjustable nozzle movement system. To increase the accuracy of the zero nozzle position determination, a technique using an electrical circuit at low voltage is proposed.

In the near future cleaning experiments of whey protein fouling will be conducted to investigate the differences between local and total cleaning time at different wavinesses.

## NOMENCLATURE

### Symbols

- $B$  Boltzmann constant,  $\text{kg s}^{-1}$
- $d$  diameter, m
- $d_t$  inner diameter of nozzle, m
- $dx$  Boltzmann time constant
- $h$  distance between nozzle tip and deposit layer, m
- $h_0$  distance between nozzle tip and substrate surface, m
- $l$  length, m
- $\dot{m}$  discharge mass flow rate through the nozzle,  $\text{kg s}^{-1}$
- $P$  pressure, Pa
- $\dot{q}$  heat flux,  $\text{W m}^{-2}$
- $R^2$  correlation coefficient, dimensionless
- $Re$  Reynolds number,  $Re = w d_n / \nu$ , dimensionless
- $s$  width of nozzle rim, m
- $T$  temperature, K
- $t$  Time, s
- $u$  uncertainty
- $W$  waviness,  $w_{os,max} / \bar{w}$ , dimensionless
- $w$  flow velocity,  $\text{m s}^{-1}$
- $\bar{w}$  mean flow velocity,  $\text{m s}^{-1}$
- $\chi_c$  Boltzmann constant center

### Greek symbols

- $\alpha$  nozzle inner angle, rad
- $\delta$  deposit thickness, m

$\lambda$	length of nozzle exit, m
$\nu$	kinematic viscosity, $\text{kg s}^{-1} \text{m}^{-1}$
$\rho$	density, $\text{kg m}^{-3}$
$\tau$	cleaning time, s
$\omega$	angular frequency, $\text{s}^{-1}$

**Subscripts**

<i>annulus</i>	annulus
<i>bulk</i>	bulk
<i>e</i>	end/final
<i>h</i>	hydraulic
<i>M</i>	main
<i>m</i>	measurement
<i>max</i>	maximal
<i>os</i>	oscillating
<i>stat</i>	stationary
<i>w</i>	wall
0	initial

**Acronyms**

CCD	Charge-coupled device
CFD	Computational fluid dynamics
CIP	Cleaning-in-place
FDG	Fluid dynamic gauging

**REFERENCES**

- Augustin, W., and Bohnet, M., 1999, Influence of pulsating flow on fouling behaviour, *Proc. Int. Conference on Mitigation of Heat Exchanger Fouling and its Economic and Environmental Implications*, Banff, Canada, pp. 161-168.
- Augustin, W., Fuchs, T., Föste, H., Schöler, M., Majschak, J.-P., and Scholl, S., 2010, Pulsed flow for enhanced cleaning in food processing, *Food Bioprod. Process.*, Vol. 88, pp. 384-391.
- Bode, K., Hooper, R. J., Paterson, W. R., Wilson, D. I., Augustin, W., and Scholl, S., 2007, Pulsed flow cleaning of whey protein fouling layers, *Heat Transfer Eng.*, Vol. 28, No. 3, pp. 202-209.
- Dürr, H., and Wildbrett, G., 2006, Reinigungsvorgänge – Verfahrensparameter und ihr Wirkungen, in *Reinigung und Desinfektion in der Lebensmittelindustrie*, eds. Wildbrett, G., 2nd ed., Behr's Verlag, Hamburg, pp. 94-112.
- Föste, H., Schöler, M., Majschak, J.-P., Augustin, W., and Scholl, S., 2013, Modeling and validation of the mechanism of pulsed flow cleaning, *Heat Transfer Eng.*, Vol. 34, No. 8-9, pp. 753-760.
- Fryer, P. J., and Asteriadou, K., 2009, A prototype cleaning map: A classification of industrial cleaning processes, *Trends Food Sci. Technol.*, Vol. 20, No. 6-7, pp. 255-262.
- Gillham, C. R., Fryer, P. J., Hasting, A. P. M., and Wilson, D. I., 2000, Enhanced cleaning of whey protein soils using pulsed flows, *J. Food Eng.*, Vol. 46, pp. 199-209.
- Goode, K. R., Asteriadou, K., Robbins, P. T., and Fryer, P. J., 2013, Fouling and cleaning studies in the food and beverage industry classified by cleaning type, *Compr. Rev. Food Sci. Food Saf.*, Vol. 12, pp. 121-143.
- Gu, T., Chew, Y. M. J., Paterson, W. R., and Wilson, D. I., 2009, Experimental and CFD studies of fluid dynamic gauging in annular flows, *AIChE Journal*, Vol. 55, No. 8, pp. 1937-1947.
- Gu, T., Albert, F., Augustin, W., Chew, Y. M. J., Mayer, M., Paterson, W. R., Scholl, S., Sheikh, I., Wang, K., and Wilson, D. I., 2011, Application of fluid dynamic gauging to annular test apparatuses for studying fouling and cleaning, *Exp. Therm Fluid Sci.*, Vol. 35, pp. 509-520.
- Schlichting, H., and Gersten, K., 2006, Grundzüge der Grenzschichttheorie, in *Grenzschichttheorie*, eds. Schlichting, H., and Gersten, K., 10th ed., Springer-Verlag, New York, pp. 27-48.
- Schöler, M., Fuchs, T., Helbig, M., Augustin, W., Scholl, S., and Majschak, J.-P., 2009, Monitoring of the local cleaning efficiency of pulsed flow cleaning procedures, *Proc. 9<sup>th</sup> Int. Conference on Heat Exchanger Fouling and Cleaning*, Schladming, Austria, pp. 161-168.
- Tuladhar, T. R., Paterson, W. R., Macleod, N., and Wilson, D. I., 2000, Development of a novel non-contact proximity gauge for thickness measurement of soft deposits and its application in fouling studies, *Can. J. Chem. Eng.*, Vol. 78, pp. 935-947.
- Wang, S., Schlüter, F., Gottschalk, N., Scholl, S., Wilson, D. I., and Augustin, W., 2016, Aseptic Zero Discharge Fluid Dynamic Gauging for Measuring the Thickness of Soft Layers on Surfaces, *Chem. Ing. Tech.*, Vol. 88, No. 10, pp. 1530-1538.